Micron-scale copper wires printed using femtosecond laser-induced forward transfer with automated donor replenishment

James A. Grant-Jacob,[1,*] Benjamin Mills,[1] Matthias Feinaeugle,[1] Collin L. Sones,[1] Gerrit Oosterhuis,[2] Marc B. Hoppenbrouwers,[3] and Robert W. Eason[1]

[1]*Optoelectronics Research Centre, University of Southampton, Southampton, UK*
[2]*TNO Science and Industry, P.O. Box 6235, 5600 HE, Eindhoven, The Netherlands*
[3]*Holst Centre/TNO, High Tech Campus 31, 5656 AE Eindhoven, The Netherlands*
**jagj1v11@soton.ac.uk*

Abstract: We demonstrate the use of laser-induced forward transfer (LIFT) in combination with a novel donor replenishment scheme to print continuous copper wires. Wires of mm length, a few microns wide and sub-micron in height have been printed using a 800 nm, 1 kHz repetition rate, 150 fs pulsed laser. A 120 nm thick copper donor was used along with laser pulse energy densities of 0.16-0.21 J cm^{-2} to print overlapping few-micron sized pads to form the millimeter long wires. The wires have a measured resistivity of 17 ± 4 times that of bulk copper.

OCIS codes: (140.7090) Ultrafast lasers; (220.4000) Microstructure fabrication; (220.4241) Nanostructure fabrication; (220.4610) Optical fabrication; (350.3390) Laser materials processing.

References and links

1. T. Jung and A. Westphal, "Zirconia thin film deposition on silicon by reactive gas flow sputtering: the influence of low energy particle bombardment," Mater. Sci. Eng. A **140**, 528–533 (1991).
2. R. C. Jaeger, *Introduction to Microelectronic Fabrication: Volume 5 of Modular Series on Solid State Devices* (Prentice Hall 2002), Chap. 6.
3. J. Käshammer, P. Wohlfart, J. Weiß, C. Winter, R. Fischer, and S. Mittler-Neher, "Selective gold deposition via CVD onto self-assembled organic monolayers," Opt. Mater. **9**(1-4), 406–410 (1998).
4. J. A. M. Sondag-Huethorst, H. R. J. van Helleputte, and L. G. J. Fokkink, "Generation of electrochemically deposited metal patterns by means of electron beam (nano) lithography of self-assembled monolayer resists," Appl. Phys. Lett. **64**(3), 285–287 (1994).
5. S. A. Boden, Z. Moktadir, D. M. Bagnall, H. Mizuta, and H. N. Rutt, "Focused helium ion beam milling and deposition," Microelectron. Eng. **88**(8), 2452–2455 (2011).
6. J. Bohandy, B. F. Kim, and F. J. Adrian, "Metal deposition from a supported metal film using an excimer laser," J. Appl. Phys. **60**(4), 1538–1539 (1986).
7. D. P. Banks, C. Grivas, J. D. Mills, R. W. Eason, and I. Zergioti, "Nanodroplets deposited in microarrays by femtosecond Ti:sapphire laser-induced forward transfer," Appl. Phys. Lett. **89**(19), 193107 (2006).
8. E. Fogarassy, C. Fuchs, F. Kerherve, G. Hauchecorne, and J. Perriere, "Laser-induced forward transfer of high-T_c YBaCuO and BiSrCaCuO superconducting thin films," J. Appl. Phys. **66**(1), 457–459 (1989).
9. H. Kim, G. P. Kushto, C. B. Arnold, Z. H. Kafafi, and A. Pique, "Laser processing of nanocrystalline TiO_2 films for dye-sensitized solar cells," Appl. Phys. Lett. **85**(3), 464–466 (2004).
10. P. Papakonstantinou, N. A. Vainos, and C. Fotakis, "Microfabrication by UV femtosecond laser ablation of Pt, Cr and indium oxide thin films," Appl. Surf. Sci. **151**(3-4), 159–170 (1999).
11. D. A. Willis and V. Grosu, "Microdroplet deposition by laser-induced forward transfer," Appl. Phys. Lett. **86**(24), 244103 (2005).
12. I. Zergioti, S. Mailis, N. A. Vainos, P. Papakonstantinou, C. Kalpouzos, C. P. Grigoropoulos, and C. Fotakis, "Microdeposition of metal and oxide structures using ultrashort laser pulses," Appl. Phys., A Mater. Sci. Process. **66**(5), 579–582 (1998).
13. A. I. Kuznetsov, R. Kiyan, and B. N. Chichkov, "Laser fabrication of 2D and 3D metal nanoparticle structures and arrays," Opt. Express **18**(20), 21198–21203 (2010).
14. M. L. Tseng, C. M. Chang, B. H. Chen, Y. W. Huang, C. H. Chu, K. S. Chung, Y. J. Liu, H. G. Tsai, N. N. Chu, D. W. Huang, H. P. Chiang, and D. P. Tsai, "Fabrication of plasmonic devices using femtosecond laser-induced forward transfer technique," Nanotechnology **23**(44), 444013 (2012).
15. A. I. Kuznetsov, C. Unger, J. Koch, and B. N. Chichkov, "Laser-induced jet formation and droplet ejection from thin metal films," Appl. Phys., A Mater. Sci. Process. **106**(3), 479–487 (2012).

#187377 - $15.00 USD Received 19 Mar 2013; revised 3 May 2013; accepted 5 May 2013; published 8 May 2013

16. M. Kandyla, S. Chatzandroulis, and I. Zergioti, "Laser induced forward transfer of conducting polymers," Opto-Electron. Rev. **18**(4), 345–351 (2010).
17. P. Serra, M. Colina, J. M. Fernández-Pradas, L. Sevilla, and J. L. Morenza, "Preparation of functional DNA microarrays through laser-induced forward transfer," Appl. Phys. Lett. **85**(9), 1639–1641 (2004).
18. P. Serra, J. M. Fernández-Pradas, F. X. Berthet, M. Colina, J. Elvira, and J. L. Morenza, "Laser direct writing of biomolecule microarrays," Appl. Phys., A Mater. Sci. Process. **79**(4-6), 949–952 (2004).
19. D. A. Willis and V. Grosu, "Evaporation and phase explosion during laser-induced forward transfer of aluminium," Proc. SPIE **5339**, 304–312 (2004).
20. M. Feinaeugle, A. P. Alloncle, Ph. Delaporte, C. L. Sones, and R. W. Eason, "Time-resolved shadowgraph imaging of femtosecond laser-induced forward transfer of solid materials," Appl. Surf. Sci. **258**(22), 8475–8483 (2012).
21. C. L. Sones, K. S. Kaur, P. Ganguly, D. P. Banks, Y. J. Ying, R. W. Eason, and S. Mailis, "Laser-induced-forward-transfer: a rapid prototyping tool for fabrication of photonic devices," Appl. Phys., A Mater. Sci. Process. **101**(2), 333–338 (2010).
22. B. Hopp, T. Smausz, Z. Antal, N. Kresz, Z. Bor, and D. Chrisey, "Absorbing film assisted laser induced forward transfer of fungi (Trichoderma conidia)," J. Appl. Phys. **96**(6), 3478–3481 (2004).
23. G. Oosterhuis, B. H. in't Veld, G. Ebberink, D. A. del Cerro, E. van den Eijnden, P. Chall, and B. van der Zon, "Additive interconnect fabrication by picosecond Laser Induced Forward Transfer," in 3D Systems Integration Conference (3DIC), 2010 IEEE International (Institute of Electrical and Electronics Engineers, New York, 2010) pp. 1–5.
24. B. K. Park, D. Kim, S. Jeong, J. Moon, and J. S. Kim, "Direct writing of copper conductive patterns by ink-jet printing," Thin Solid Films **515**(19), 7706–7711 (2007).
25. L. Rapp, J. Ailuno, A. P. Alloncle, and P. Delaporte, "Pulsed-laser printing of silver nanoparticles ink: control of morphological properties," Opt. Express **19**(22), 21563–21574 (2011).
26. R. C. Y. Auyeung, H. Kim, S. A. Mathews, and A. Piqué, "Laser direct-write of metallic nanoparticle inks," J. Laser Micro/Nanoeng. **2**(1), 21–25 (2007).

1. Introduction

The ability to print continuous wires of metals, such as copper, is important for a wide variety of scientific and technological applications. Current metal deposition techniques include sputtering [1], evaporation [2] and chemical vapor deposition [3], but these lack the ability to achieve micron-scale spatial resolution for patterning without additional processing steps. Other methods for surface patterning of metals and other materials, such as e-beam lithography [4] and focused ion beam assisted deposition [5], are generally very time-consuming due to the requirement of processing under vacuum conditions. An alternative technique, laser-induced forward transfer (LIFT), can be used to directly print metals via transfer from a thin-film donor to a nearby receiver using ultrashort laser pulses [6–8]. In most LIFT processing, the thin-film donor is deposited on a transparent carrier, which is used for support.

Owing to its simplicity, LIFT has gained significant attention during the last decade [9–11] for printing of materials such as metals [12–15], superconductors [8], polymers [16], and biological substances such as DNA [17] and proteins [18]. LIFT transfer can occur via a range of physical phenomena that includes pressure build-up [19,20], melt-through [21] or the use of sacrificial layers [22], where the process depends on the desired end application and the nature of the donor material to be transferred. When using film donors of ~1 μm thickness, LIFT occurs by vaporization of the surface region at the donor-carrier interface, with the resultant pressure buildup propelling the donor pellet (often referred to as the flyer [20]) towards the receiver, whereas for thin films (typically <50 nm for chromium), using optimized laser pulse energy densities, transfer can occur solely by melt-through of the entire donor source film. Under certain conditions, after appropriate process optimization, only the central region of the melted donor film can be transferred, resulting in a sub-μm diameter pad, even though the melted region can be approximately one order of magnitude larger, hence allowing printing of features that can be ~100 times smaller in area than the spot-size of the incident laser pulse [11].

Ultrashort pulse lasers can operate at repetition rates that span many 10's of MHz for pulse energies of order a few nJ, to the ~1 kHz rate for ~1 mJ pulses. For most LIFT processing, the typical energy fluence required is between 0.1 – 1 J cm^{-2} at the donor surface, which leads to LIFTed features that have maximum areas of ~10^{-3} cm^2 when using single pulses. The benefit

#187377 - $15.00 USD Received 19 Mar 2013; revised 3 May 2013; accepted 5 May 2013; published 8 May 2013

of high repetition rate printing is that features such as pads with an area equivalent to ~1 cm^2 or wires of 100 µm x 1 m could theoretically be printed in only 1 s.

As has been convincingly shown by Willis and Grosu [11], there is considerable material damage incurred to the donor when transfer is by melt-through. As shown in the schematic in Fig. 1, a sufficiently large distance must be introduced between subsequent depositions so that LIFT is not attempted from previously exposed donor areas. In practice this may be of order one spot diameter, but even then, in our experience, precise forward LIFT does not always occur.

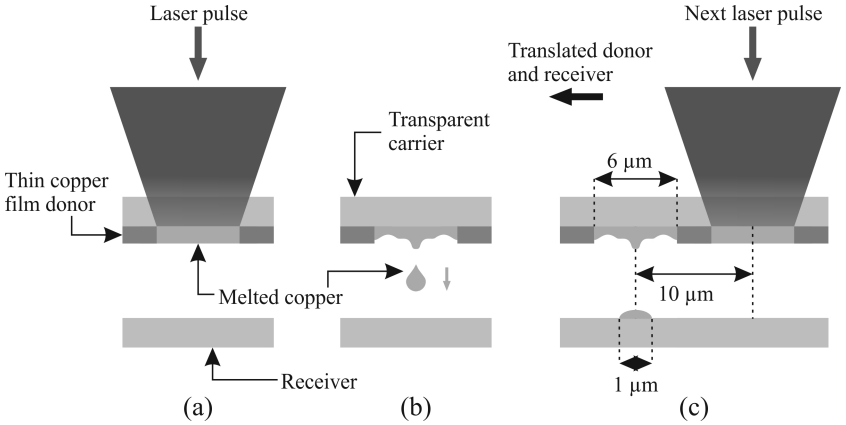

Fig. 1. Schematic of a non-donor-replenishment LIFT process, with parameters used in this work. (a) A laser pulse melts region of copper, (b) melted copper drop attaches to receiver and (c) donor and receiver are translated beneath laser so that a fresh region of copper is available for the next laser pulse.

Although printing of copper lines [6] has previously been demonstrated using LIFT, (in fact Cu was one of the very first published LIFT results), wires were LIFTed from a single composite carrier + donor + receiver sandwich structure. Inevitably this method of printing wires results in both defects and discontinuities as splashing can occur from the molten metal impinging on the surface of the receiver. What is needed is a scheme of donor replenishment, whereby fresh donor can be supplied to fill in gaps within the previously printed regions, thereby ensuring continuous features with the correct amount of infill and overlap. Oosterhuis *et al.* [23] have demonstrated the fabrication of 1 cm long, ~20 µm wide and over 1 µm high copper wires using picosecond LIFT. In this work, we demonstrate the fabrication of millimeter long wires with few micron-scale width and submicron scale height using femtosecond LIFT.

2. Experimental

Single ~150 fs laser pulses from a tunable ultrafast Ti:sapphire laser system operating at a central wavelength of 800 nm and a maximum average pulse energy density of ~0.2 J cm^{-2} were used in the work presented here. The laser operated in manual triggering mode, with one pulse triggered every 25 ms. A 1 mm diameter circular aperture was positioned in the path of the beam to produce a beam with a clipped-Gaussian spatial intensity profile, which was then focused onto the carrier-donor interface using a 50 x magnification microscope objective lens (Nikon, N.A. = 0.55) to produce a spot size of the focused pulse with a diameter of 6 µm.

The donor consisted of a transparent silica slide with one face coated with 120 nm of copper using thermal evaporation, while the receiver was an uncoated transparent silica slide. The donor and the receiver were separated from each other using 3 µm thick Mylar as a spacer, which resulted in ~1 µm diameter copper pads produced with single pulses. The copper-coated carrier and the receiver were placed on a computer-controlled 3-axis stage to allow accurate position of the donor and receiver in the path of the laser pulse. The donor and receiver were translated together at a velocity of 0.4 mm s^{-1} to allow the printing of one

#187377 - $15.00 USD Received 19 Mar 2013; revised 3 May 2013; accepted 5 May 2013; published 8 May 2013

copper pad every 10 μm. This lateral separation between each transferred area on the donor was to allow a new undisturbed region of the donor to be used in the LIFT process [7] (see Fig. 1) thus enabling printing of ideally similar ~1 μm copper pads. Following this first printing run, both the donor and the receiver were translated back to the original position and then the donor was translated 25 μm laterally relative to the line of pads on the receiver so that an unused region of the donor could be used for the next print run. In addition, the receiver was translated by 0.5 μm with respect to the laser focus, in the direction of the printed line, before a new set of pads were printed, so that every new copper pad would overlap the previous one by 0.5 μm, if we assume each pad was 1 μm in diameter, hence leading to two connected pads (see Fig. 2). After 10 sets of replenishments, a 1 mm line of connected ~1μm pads was produced to form a 1 mm long wire. The use of the described donor replenishment scheme is essential, as without this approach, the printed copper pads would vary significantly in size and shape, thus leading to the formation of discontinuous copper wires. Subsequently, the printed copper wire was imaged using a Carl Zeiss SMT, Inc., Evo® scanning electron microscope (SEM).

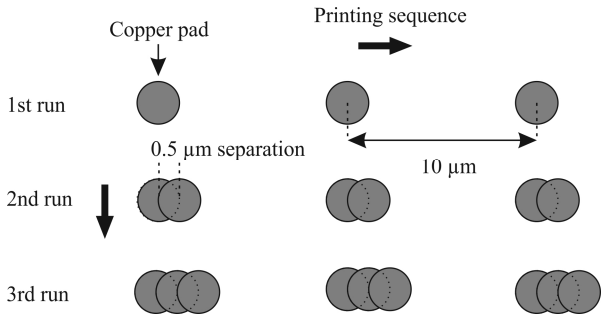

Fig. 2. Schematic of the printing overlapping process, for a 0.5 μm center-to-center pad overlap (assuming 1 μm diameter pads in the figure).

3. Results and discussion

3.1 SEM images

Figures 3(a) and 3(b) show typical single pads LIFTed at a pulse energy density of 0.16 J cm^{-2} and 0.21 J cm^{-2} respectively, each formed using a single pulse. For the conditions outlined here, the pad formed in (a) has little splatter and has a maximum diameter of 1.7 μm, while the pad in (b) is dispersed and has an irregular profile extending to ~2.5 μm. The mean of the maximum diameters of the pads at 0.16 J cm^{-2} was 1.6 μm with a standard deviation of ± 0.4 μm, while the mean of the maximum diameters of the pads at 0.21 J was 2.8 ± 0.5 μm. Using a KLA Tencor P-16 Stylus Profiler, the mean of the maximum heights of the pads for 0.16 J cm^{-2} pulse energy density was measured to be 272 ± 14 nm, while at 0.21 J cm^{-2} pulse energy density, this value was 203 ± 15 nm. From microscope images taken of the donor (see inset to Fig. 3), in the region in which the laser spot is focused on the copper donor, little copper remains after the LIFT. At lower energy densities not reported in this work, a significant amount of the material can remain on the donor, which is the case in the schematic in Fig. 1. The percentage of copper that is successfully transferred to the receiver as a pad in the LIFT process at a laser pulse energy density of 0.16 J cm^{-2} is ~35%.

#187377 - $15.00 USD Received 19 Mar 2013; revised 3 May 2013; accepted 5 May 2013; published 8 May 2013

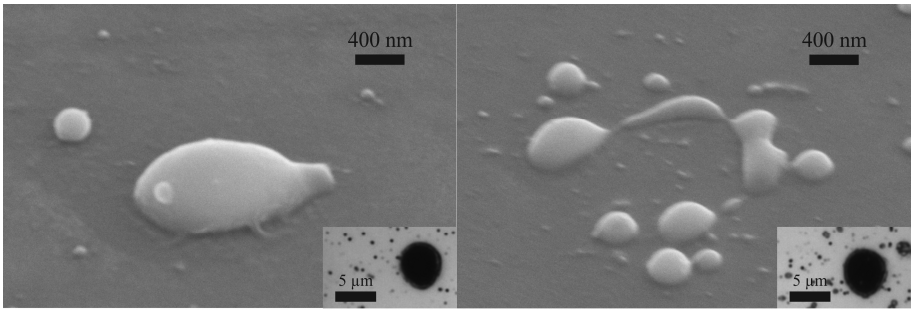

(a) (b)

Fig. 3. SEM images of (a) a smooth pad and (b) a broken pad. The SEM images were taken at 45°. Inset: microscope images of the donor after LIFT of a pad.

The results of printing continuous wires of copper using different laser pulse energy densities and center-to-center pad separation are shown in Fig. 4. The figure shows a continuous wire printed using a laser pulse energy density of 0.16 J cm^{-2} (Figs. 4(a) and 4(b)) and 0.21 J cm^{-2} (Figs. 4(c) and 4(d)), with a center-to-center pad separation of 1 µm (Figs. 4(a) and 4(c)) and 0.5 µm (Figs. 4(b) and 4(d)) From top view SEM imaging of the wires, the mean width of the wire in (a) was measured to be 1.2 ± 0.4 µm, smaller than the 2.3 ± 0.3 µm width of the wire in (b). This is due to the reduced pad overlap in the production of the wire in (a). This is also evident at a higher pulse energy density of 0.21 J cm^{-2}, the width of the wire at 1 µm center-to-center pad separation (c) being 2.5 ± 0.5 µm, whereas the width of the wire at 0.5 µm center-to-center pad separation (d), is 3.3 ± 0.3µm. At a pulse energy density of 0.21 J cm^{-2}, the wires are much wider compared with the equivalent center-to-center pad separation at a lower pulse energy density of 0.16 J cm^{-2} for the equivalent pad separation. The larger pad diameter, wire width and greater splatter at higher pulse energy density is due to a greater volume on the donor being above threshold for LIFT and the LIFTed copper moving at higher speed. Using the Stylus profiler, the mean height of the wire shown in (a) was measured to be 833 ± 64 nm, while for (b) was 1083 ± 250 nm, (c) was 828 ± 93 nm and (d) was 1018 ± 117 nm. Although at 0.21 J cm^{-2} laser pulse energy density the pads are broken, since the mean diameter of the pads is greater than twice the center-to-center pad separation of 1 µm, then the pads will overlap each other a multiple of times by varying amounts during the printing of the wire, thus leading to a continuous wire of copper. In addition, a pad undergoing LIFT will be partly printed onto other pads rather than onto a virgin flat glass surface (as in the case of pads in Fig. 3), thus resulting in slightly different pad formation and wire width.

#187377 - $15.00 USD Received 19 Mar 2013; revised 3 May 2013; accepted 5 May 2013; published 8 May 2013

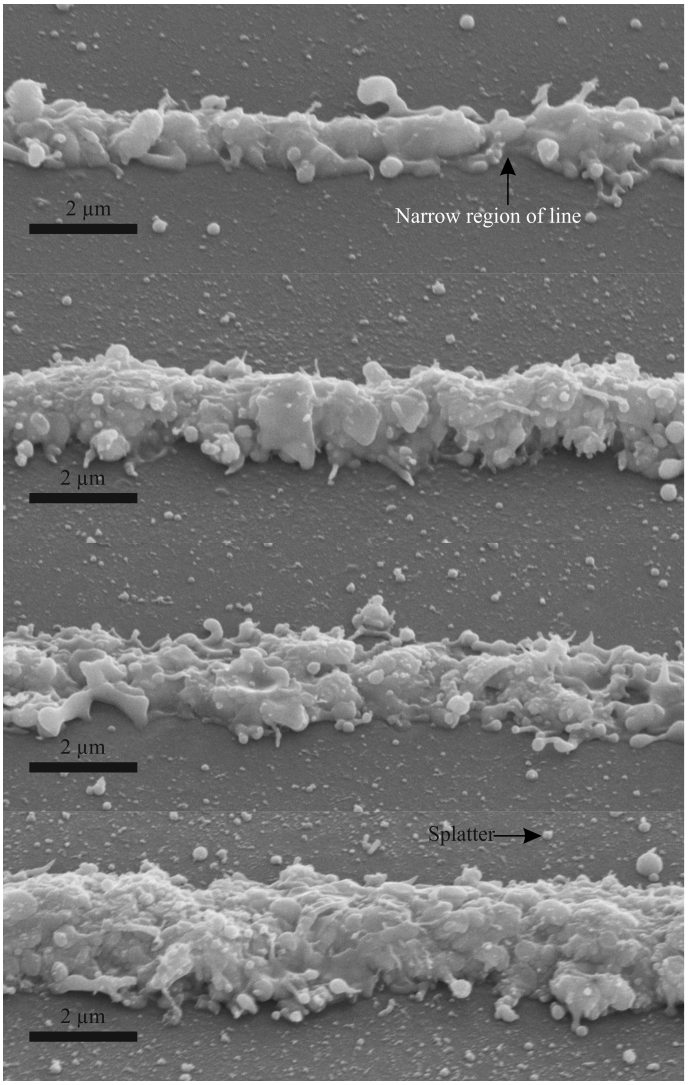

Fig. 4. SEM images of sections of continuous wires of copper printed using a laser pulse energy density of (a) 0.16 J cm^{-2} with 1 µm center-to-center pad separation, (b) 0.16 J cm^{-2} with 0.5 µm center-to-center pad separation, (c) 0.21 J cm^{-2} with 1 µm center-to-center pad separation and (d) 0.21 J cm^{-2} with with 0.5 µm center-to-center pad separation. The SEM images were taken at 45°.

Figure 5 shows a top-view SEM image of the entire copper wire we were able to produce with a laser pulse energy density of 0.16 J cm^{-2} and a 0.5 µm center-to-center pad separation. This is the smoothest, narrowest wire that has the least amount of splatter that we were able to produce. The image shows a continuous 1 mm wire of copper on a transparent silica slide, with an inset to the figure showing a zoomed-in image of the copper wire. The total time taken to produce the wires was 10 minutes, which was dependent on the speed of stage translation, the length of the wire, the size of the pad, the center-to-center pad separation and the size of the ablated region on the donor. During probe measurements described in section 3.2, the wires remained intact unless the probes were moved across the wires, in which case the line would break and the piece of the wire that was in contact with the probe would break away from the wire.

#187377 - $15.00 USD Received 19 Mar 2013; revised 3 May 2013; accepted 5 May 2013; published 8 May 2013

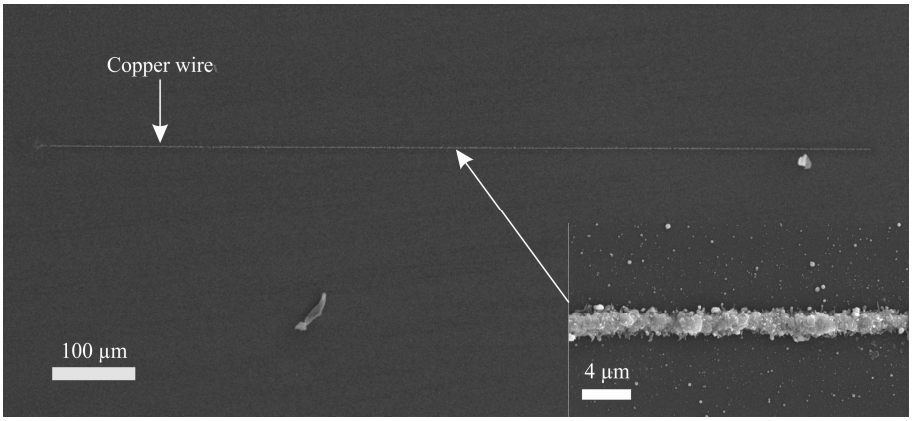

Fig. 5. SEM image of a continuous 1 mm long copper wire for laser pulse energy density of 0.16 J cm^{-2}, produced using a 0.5 μm center-to-center pad separation.

3.2 Electrical characterization

To verify the structural continuity of the copper wire shown in Fig. 5, the resistance of the wire was measured using an Agilent 4155C Semiconductor Parameter Analyzer with a Cascade Microtech DC probe station. A single measurement gave the resistance as 238 ± 9 Ω and the resistivity, ρ, is calculated using $\rho = RA / L$, where R is the resistance, A is the cross-sectional area and L is the length of the wire, and is calculated to be 3.2 ± 0.7 x 10^{-7} Ω m, which is 17 ± 4 times larger than the resistivity of bulk copper (1.72 x 10^{-8} Ω m). We attribute this difference to the fact that we have assumed a constant cross-sectional area of the wire in our calculations, which has been calculated from Stylus Profiler measurements, as a full measurement would be impractical. In practice, due to the fabrication process, and as evident in the presented SEM images, the wire width and height can vary considerably (~23%) and can include narrow regions (see Fig. 4(a) for an example), which will increase the local resistivity of the wire. An important point to note here is that there was no conductivity detected between the wires. Future work will concentrate on the optimization of the fabrication process and should hence improve the wire quality. However, such an increased value of resistivity is expected, given the large number of pads (2000) that we combined together to produce the wire in Fig. 5, as each pad may well have additional undesirable copper oxide (an electrical insulator) as an impurity constituent, which would certainly contribute to the local resistance. The copper oxide is present on the surface of the donor before LIFT and will form on the surface of the droplet during and after LIFT. Indeed, EDX (energy-dispersive X-ray spectroscopy) analysis of the copper wire has shown that the ratio of copper atoms to oxygen atoms was 2:1, thus indicating a significant amount of copper oxide present. To date, alternative methods such as ink-jet printing of copper have produced 40 μm wide wires with resistivities 1000 times that of bulk copper [24] and the laser direct write of silver nanoparticle inks has produced wire widths of approximately 20 μm, with resistivities 5-10 times that of bulk silver [25,26].

4. Conclusion

In conclusion, we have demonstrated the successful fabrication of continuous copper micro-wires using femtosecond LIFT with automated donor replenishment. One of the 1 mm wires we have printed is ~800 nm high and ~1 μm wide. At a laser pulse energy density of 0.16 J cm^{-2}, the pads were smaller with the least amount of splatter compared with pads produced using 0.21 J cm^{-2} laser pulse energy density, leading to narrower copper wires. Future work will concentrate on the optimization of the overlap parameters as well as reducing the amount of splatter. The results published here could lead to rapid microstructure fabrication of

#187377 - $15.00 USD Received 19 Mar 2013; revised 3 May 2013; accepted 5 May 2013; published 8 May 2013

complex 3D structures in micro and nanotechnology as well as application to optical materials and devices.

Acknowledgments

The authors are grateful to the EU Seventh Framework Programme for funding under the grant, e-LIFT (247868-FP7-ICT-2009-4), and to the Engineering and Physical Sciences Research Council (EPRSC) under grant no. EP/J008052/1.

#187377 - $15.00 USD Received 19 Mar 2013; revised 3 May 2013; accepted 5 May 2013; published 8 May 2013